Science of the Total Environment 904 (2023) 166857

Contents lists available at ScienceDirect

Science of the Total Environment

journal homepage: www.elsevier.com/locate/scitotenv

Establishing an emission inventory for ammonia, a key driver of haze formation in the southern North China plain during the COVID-19 pandemic

Shili Yang [a], Mingya Wang [a], Wenju Wang [a], Xuechun Zhang [a], Qiao Han [b,c,*], Haifeng Wang [d], Qinqing Xiong [a], Chunhui Zhang [a], Mingshi Wang [a,*]

[a] College of Resource and Environment, Henan Polytechnic University, Jiaozuo 454003, China
[b] Institute of Geochemistry, Chinese Academy of Sciences, 550081 Guiyang, China
[c] University of Chinese Academy of Sciences, Beijing 100049, China
[d] Jincheng Ecological Environment Bureau, Jincheng 048000, China

HIGHLIGHTS

- Total NH_3 emissions were only reduced by about 4 % in 2020 compared to 2019.
- Non-agricultural sources were more severely influenced than agricultural sources.
- Percentage of NH_3 emissions from livestock at four manure management stages.
- Checking for random annual variations, Monte Carlo simulation uncertainty analysis.

GRAPHICAL ABSTRACT

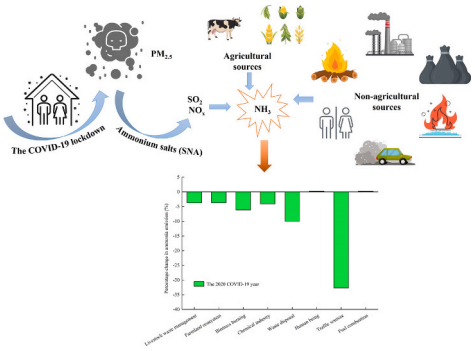

ARTICLE INFO

Editor: Pavlos Kassomenos

Keywords:
COVID-19
NH_3 emission inventory
Inter-annual variation
Spatial distribution
Uncertainty analysis

ABSTRACT

Despite the significant reduction in atmospheric pollutant levels during the COVID-19 lockdown, the presence of haze in the North China Plain remained a frequent occurrence owing to the enhanced formation of secondary inorganic aerosols under ammonia-rich conditions. Quantifying the increase or decrease in atmospheric ammonia (NH_3) emissions is a key step in exploring the causes of the COVID-19 haze. Historic activity levels of anthropogenic NH_3 emissions were collected through various yearbooks and studies, an anthropogenic NH_3 emission inventory for Henan Province for 2020 was established, and the variations in NH_3 emissions from different sources between COVID-19 and non-COVID-19 years were investigated. The validity of the NH_3 emission inventory was further evaluated through comparison with previous studies and uncertainty analysis from Monte Carlo simulations. Results showed that the total NH_3 emissions gradually increased from north-west to south-east, totalling 751.80 kt in 2020. Compared to the non-COVID-19 year of 2019, the total NH_3 emissions were reduced by approximately 4 %, with traffic sources, waste disposal and biomass burning serving as the sources with the top three largest reductions, approximately 33 %, 9.97 % and 6.19 %, respectively. Emissions

* Corresponding authors.
E-mail addresses: hanqiao@mail.gyig.ac.cn (Q. Han), mingshiwang@hpu.edu.cn (M. Wang).

https://doi.org/10.1016/j.scitotenv.2023.166857
Received 18 April 2023; Received in revised form 20 August 2023; Accepted 3 September 2023
Available online 9 September 2023

from humans and fuel combustion slightly increased. Meanwhile, livestock waste emissions decreased by only 3.72 %, and other agricultural emissions experienced insignificant change. Non-agricultural sources were more severely influenced by the COVID-19 lockdown than agricultural sources; nevertheless, agricultural activities contributed 84.35 % of the total NH_3 emissions in 2020. These results show that haze treatment should be focused on reducing NH_3, particularly controlling agricultural NH_3 emissions.

1. Introduction

The COVID-19 epidemic swept the world in early 2020 (Wang et al., 2020), and precise lockdowns were implemented in China to effectively curb the epidemic. Some communities, towns and urban areas were defined as medium- and high-risk regions based on infections and close contacts, and movement of people and road traffic was restricted (Tian et al., 2020), significantly decreasing the possibility of virus spread. Although economic development was severely hampered owing to a reduction in human activity, air pollutants levels significantly declined. The average decrease in SO_2, $PM_{2.5}$, PM_{10} and NO_2 levels in 44 cities in northern China was 6.76 %, 5.93 %, 13.66 % and 24.67 %, respectively (Bao and Zhang, 2020). This phenomenon occurred throughout the world, such as in India (Sekar et al., 2023); Rio de Janeiro, the second largest industrial city of Brazil (Dantas et al., 2020); and Almaty, the capital of Kazakhstan (Kerimray et al., 2020). Despite the significant drop in atmospheric pollutants levels, severe haze remained in the North China Plain and East China during the COVID-19 lockdown (Huang et al., 2021; Peng et al., 2021), and the rapid production of secondary inorganic aerosols under ammonia-rich conditions was considered to be the dominant factor (Ren et al., 2021).

Atmospheric ammonia (NH_3), the principal alkaline gas in the atmosphere (Krupa, 2003), easily reacts with acidic gases such as SO_2 and NO_x (Goebes et al., 2003). The reaction produces [$(NH_4)_2SO_4$], (NH_4HSO_4) and (NH_4NO_3), which are the major components of $PM_{2.5}$ (Battye et al., 2003; Xu et al., 2016), frequently inducing severe haze events and decreased urban visibility (Pan et al., 2018; Wang et al., 2022). Ammonium salts (NH_4^+) were the main component involved in the formation of the COVID-19 lockdown haze, accounting for 41 %–72 % of $PM_{2.5}$, and the contribution of ammonium salts to $PM_{2.5}$ rises with haze production (Chang et al., 2020; Yang et al., 2022). Moreover, NH_3 aggravates the greenhouse effect (Hellsten et al., 2008), and excessive NH_3 deposits can cause serious environmental problems such as decreased photo-biodiversity (Chen et al., 2020), soil acidification and water eutrophication (Timmer et al., 2005).

To investigate the contribution of NH_3 to regional haze and its influence mechanism, many studies have established NH_3 emission inventories in recent years (Battye et al., 2003; Olivier et al., 1998; Zhao and Wang, 1994). The USA has conducted detailed studies on forest and non-industrial sources of NH_3 (Sarwar et al., 2005), finding that more than 50 % originates from natural soil and vegetation. The UK has established an NH_3 emission inventory from agricultural sources using the latest survey data and accurate emission factors (Pain et al., 1998), indicating that approximately 50 % of the total NH_3 emissions come from cattle. Asia accounts for approximately half of the global NH_3 emissions (Bouwman et al., 1997) and approximately 70 % from agriculture. China is the largest emitter of air pollutants (Streets et al., 2003), as compared with 64 study regions in Asia. China has also established NH_3 emission inventories at different scales. In fact, the four major municipalities directly under the central government—Shanghai (Wang et al., 2015), Chongqing (Yang et al., 2011), Beijing and Tianjin (Zhou et al., 2015)—have performed studies of industrial, combustion and anthropogenic sources, respectively. Provincial-scale studies of NH_3 emissions have focused on the North China Plain (Cao et al., 2021; Huo et al., 2015; Wang et al., 2018a; Zhang et al., 2010a) and Yangtze River Delta (Huang et al., 2011; Yu et al., 2020), where livestock waste and nitrogen fertiliser-based agriculture account for over 70 % of anthropogenic sources. Kang et al. (2016), Huang et al. (2012) and Zhang et al. (2018) have studied the NH_3 sources and spatial-temporal variations in China with high precision respectively and concluded that agriculture was the major emissions source. Before the COVID-19 pandemic, NH_3 emissions studies were performed in various regions of the world (Battye et al., 2003; Kang et al., 2016; Olivier et al., 1998; Pain et al., 1998; Zhang et al., 2018); however, studies on the NH_3 emission inventory and NH_3 emissions characteristics during the pandemic have been lacking. Uncertainty analysis of the poor air quality that was present during the COVID-19 in the North China Plain demonstrate that the timely updating of NH_3 emission inventories helps to clarify secondary aerosol formation and emission influences (Li et al., 2021). Haze still occurred during the COVID-19 lockdown, despite the extremely low levels of human activity that were present. Therefore, a timely NH_3 emission inventory is a key to tackling atmospheric pollution.

The North China Plain, China, has been one of the worst haze-polluting regions throughout the years (Hu et al., 2014; Song et al., 2022), in which agricultural NH_3 is the primary source of anthropogenic emissions. Therefore, the emission factors method was adopted to estimate NH_3 emissions in Henan Province, a large agricultural province in the southern part of the North China Plain, from 2019 to 2020. An anthropogenic NH_3 emission inventory for Henan Province in 2020 was established and compared with NH_3 emissions from different sources before the lockdown. Then, the causes of changes in the NH_3 emissions were analysed, providing a powerful, scientific reference to explore the causes of haze during the COVID-19 lockdown.

2. Methodology and data

2.1. Study area and source categorisation

The 17 prefecture-level cities and 1 directly administered city, Jiyuan in Henan Province, served as the study area as shown in Fig. 1. We classified the estimated emission sources into eight categories, as follows: livestock waste management, farmland ecosystem, biomass burning, chemical industry, human being, fuel combustion, waste disposal and traffic sources.

2.2. Emission estimate method

As shown in Eq. (1),

$$E_{i,j} = \sum A_{i,j} \times EF_{i,j} \times \gamma \quad (1)$$

where i is the local city; j is source type; E is total NH_3 emissions; A is activity level; EF is emission factor and γ is conversion factor of N-NH_3 emissions, 1.214 for livestock and 1.0 for others. The emission factors were selected mainly based on three guidelines (MEP, 2014a, 2014b, 2014c) and applied in various domestic and international research studies(Battye et al., 2003; Huang et al., 2012; Wang et al., 2018a, 2018b; Zheng et al., 2014).

2.2.1. Livestock waste management

Based on Huang et al. (2012), breeding methods were classified into three categories: free-range, intensive and grazing. The manure management phase consisted of four stages: outdoor, housing, manure storage and treatment and subsequent fertilisation (Webb and Misselbrook, 2004), and the total ammoniacal nitrogen for each stage was calculated based on the literature (MEP, 2014a), split into solid and

liquid forms. The contribution of free-range and grazing livestock excreta was 50 % indoors and 50 % outdoors, whereas the contribution of intensive farming was 100 % indoors and 0 % outdoors (MEP, 2014a; Wang et al., 2018a, 2018b; Zhang et al., 2010a, 2010b). In this study, the livestock waste management sources were classified into 10 categories: beef cattle, dairy cattle, goats, sheep, meat pigs, sows, laying hens, laying ducks, broilers and meat ducks. The activity level data were obtained from China Statistical Yearbooks, Henan Provincial Statistical Yearbooks and various local yearbooks of Henan Province. For livestock with a breeding cycle of less than one year, year-end slaughter figures were used as estimates. For livestock and poultry with a breeding cycle greater than one year, year-end stock numbers were used as estimates (information supplemented in Tables S1, S2 and Texts S1, S2). Referring to previous research results, Eq. (2) can be used to calculate the number of poultry and egg stocks at the end of the year,

$$A_i = \frac{O_i}{N_i \times M_i} \times 10^6, \tag{2}$$

where A is the number of poultry stocks at the end of the year, pcs.; i refers to laying hens or ducks; O is the total egg production; M is the average individual egg mass, g unit^{-1}; and N is the average annual number of eggs laid by poultry, pcs.

2.2.2. Farmland ecosystem

(1) Nitrogen fertiliser application

Studies have shown that 10 %–30 % of the applied N was lost through NH_3 volatilisation (Ju et al., 2009), and the degree of NH_3 volatilisation depends on the type of fertiliser applied. Here, according to Huang et al. (2012) and Zhang et al. (2011), nitrogen fertilisers were classified into five categories: urea, ammonium bicarbonate, ammonium nitrate, ammonium sulfate and other nitrogen-containing fertilisers. Ammonia volatilisation is influenced by the type of nitrogen fertiliser used, ambient temperature, rainfall, pH level and fertiliser application method (Bouwman et al., 1997; Zhang et al., 2011). From Zhang et al. (2011), the share of application of different types of N fertilisers was obtained, as shown in Table S4. According to MEP (2014a), the NH_3 emission factor for nitrogen fertiliser application was calculated by Eq. (3),

$$EF = EF_{basis} \times a \times b, \tag{3}$$

where EF_{basis} is the baseline emission factor, a is the correction factor for the fertiliser application rate and b is the fertiliser application mode correction factor. EF_{basis} is determined by the average soil surface temperature and soil type (Bouwman et al., 1997), whereby most of the soils are neutral and slightly alkaline while a few in Henan Province are acidic (Wang et al., 2018a). The correction factor a is 1.18 if the area is fertilised above 13 kg N per acre and 1 if it is fertilised below 13 kg N. For correction factor b, 0.32 is taken for base fertiliser application and 1.0 for topdressing fertiliser application. Considering that the main crops in Henan Province are wheat, rice and maize, the average value of the different base/topdressing ratios for each crop was taken to be 1:0.48 for the ammonium bicarbonate base/topdressing ratios and 1:3.46 for the base/topdressing ratios of urea and other nitrogen fertilisers.

(2) Nitrogen-fixing plants

The primary nitrogen-fixing plants in Henan Province are soybean and peanut, and the activity level data were obtained from plant sown areas, yielding emission factors of 1.05 kg (hm a)$^{-1}$ and 1.2 kg (hm a)$^{-1}$, respectively (MEP, 2014a).

(3) Soil cultivation

Activity level data were taken from the area of arable land in the municipalities, yielding a soil ammonia volatilisation factor of 1.8 kg (hm a)$^{-1}$ (MEP, 2014a).

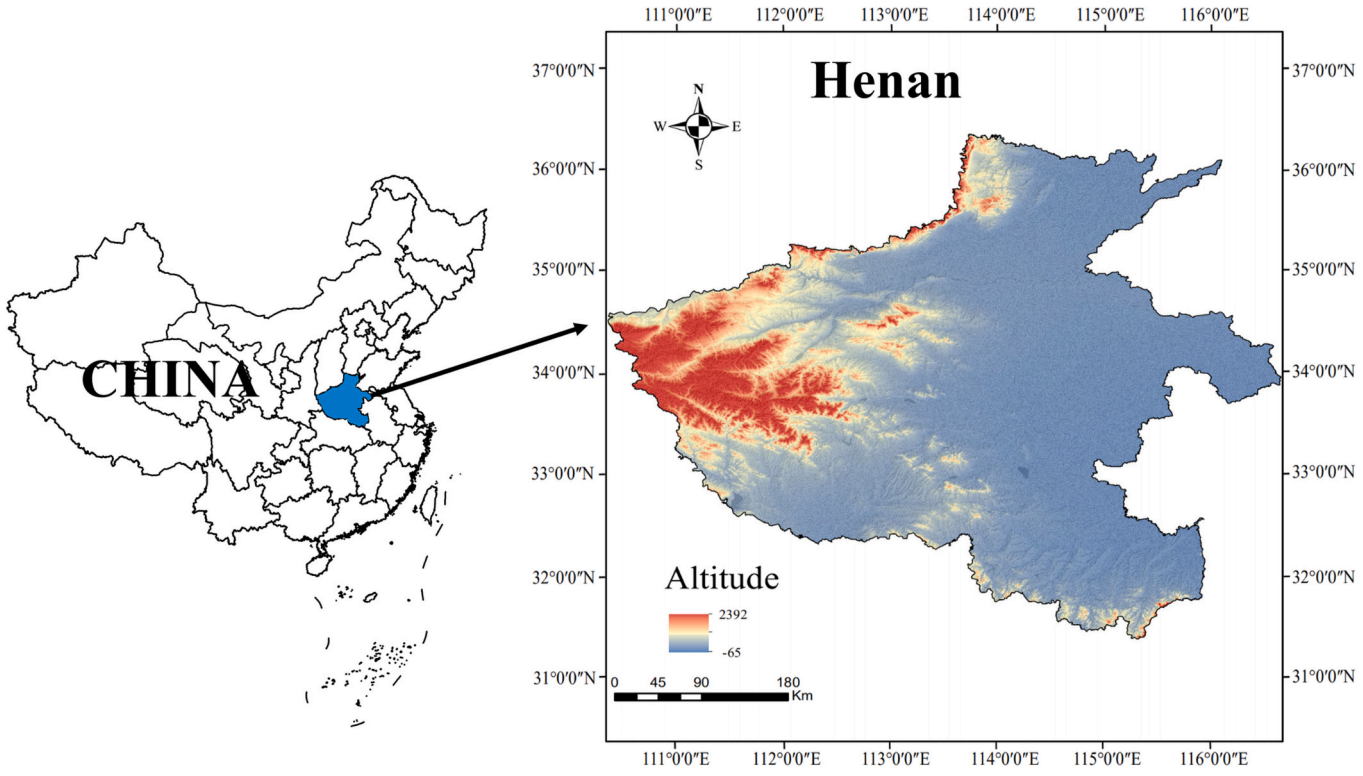

Fig. 1. Regional distribution map of cities in Henan Province.

(4) Straw composting

The amount of straw produced was obtained based on Eq. (4). Considering that the proportion of straw composted in Henan Province was 15.6 % (Ministry Of Finance, 2011), the emission factor (in terms of straw) was calculated as 0.32 kg t^{-1} from

$$A = P_j \times N_j \times Y \quad (4)$$

where A is the amount of straw burned; j is the crop type, P is the crop production of j; N is the cereal-to-grass ratio of crop j; Y is the proportion of crop waste straw composted of j.

2.2.3. Biomass burning

Biomass burning was characterised into four main forms: domestic burning of firewood, domestic burning of straw, open burning of straw and forest-fire burning. The open burning of straw calculation was based on the different crop yields in each city according to MEP (2014b) as in Eq. (5),

$$A_j = \sum P_j \times N_j \times R_j \times D_j \times Y, \quad (5)$$

where A is the amount of straw burned; j is the crop type; P is the crop yield; N is the cereal-to-grass ratio; R is the percentage of straw burned, generally taken as 20 % and Y is the burning efficiency, generally taken as 90 %. Other parameters were selected as shown in the supplemental Table S5.

The forest-fire burn consumption was calculated by Eq. (6),

$$A = AR \times D \times Y, \quad (6)$$

where AR is the fire damage area, m^2; D is the dry forest biomass, 5.5 kg m^{-2} in the warm temperate zone and Y is the burning rate, generally taken as 50 %. To obtain the total area of fire damage in Henan Province, emissions were ultimately assigned to each city based on the percentage of forested land area in each city, considering the different areas of damage in each city according to Statistical Yearbook of Henan Province.

2.2.4. Chemical industry

NH_3 emissions from chemical production are mainly derived from ammonia and fertiliser production, with activity level data taken from the Statistical Yearbook of Henan Province for each municipality (emission factors are shown in Table S6).

2.2.5. Waste disposal

NH_3 emissions from wastewater treatment processes originate mainly from the absorption and digestion of wastewater nutrient treatment processes by activated sludge microorganisms, and waste disposal forms are classified as landfills and incineration (Zhang et al., 2010a, 2010b). In Henan Province in 2020, the sanitary landfill disposal volume of domestic waste was 607.8 million t and the incineration disposal volume was 117.6 million t (HNBSB, 2021), accounting for 83.8 % and 16.2 % of the waste disposal volume, respectively. The total volume was distributed to municipalities with this proportion, using a top-down approach (emission factors are shown in Table S6).

2.2.6. Human being

Human-generated NH_3 emissions are derived mainly from faecal and urinary excretion volatilisation. Considering the low penetration of toilets in rural areas, faecal and urinary NH_3 emissions from rural areas were estimated, and the emission factor was taken as 0.787 kg (person a)$^{-1}$ (MEP, 2014a).

2.2.7. Traffic sources

Three-way catalysts (TWCs) have been used in vehicles since the 1980s to greatly reduce pollution emissions from vehicle exhausts (Frey and Zheng, 2002); however, NH_3 is an unintended emission consequence of the use of TWCs for NOx reduction. There are two major traffic sources of NH_3 emissions, catalyst-equipped gasoline vehicles and light- and heavy-duty diesel vehicles that rely on selective catalytic reduction (SCR) (Farren et al., 2020). In recent years, with the rapid growth of motor vehicle ownership in China, traffic sources have been recognised as a major source of urban NH_3 emissions (Wang et al., 2015).

NH_3 emission factors were classified into five categories, namely, light gasoline, light diesel, heavy gasoline, heavy diesel and motorcycle, based on vehicle type and fuel type. NH_3 emissions were estimated based on sub-vehicle ownership, average annual mileage and emission factors (Zheng et al., 2014), following Eq. (7). The holdings were obtained from the Henan Provincial Statistical Yearbook for each city and further subdivided with the fleet-fuel-type allocation ratio to obtain the sub-fuel-type holdings. Furthermore, the sub-model mileage data refer to the literature (MEP, 2014c) for local research data. The emission factors are shown in Table S7, and the average annual mileage of the vehicle type is shown in Table S8.

$$E_i = \sum 10^{-6} \times P_j \times M_j \times ef_j, \quad (7)$$

where E is the emissions, t; i is the region; j is the vehicle type; P is the vehicle ownership by vehicle type, units; M is the average annual mileage by vehicle type, km and ef is the emission factor by car type, g (km unit)$^{-1}$.

2.2.8. Fuel combustion

Fuel combustion was divided into industrial and domestic coal combustion, fuel oil and natural gas combustion, according to the fuel types and department used. Civil fuel combustion was estimated based on the statistical yearbook to obtain the annual per capita domestic energy consumption in Henan Province, combining with the resident populations in each city. Industrial fuel combustion was calculated from the total energy consumption of Henan Province subtracted from the total domestic energy consumption (Wang et al., 2018a), which was distributed top-down to the city-scale level according to the total value of the secondary industry in each city (emission factors are shown in Table S9).

2.3. Spatial distribution

To visually display the estimated NH_3 emissions and NH_3 emission intensity, we mapped the spatial distribution of NH_3 emissions and NH_3 emission intensity in each city of Henan Province using ArcGIS software version 10.8. Kriging interpolation was used, which interpolates based on a statistical method by calculating the spatial correlation between data points (Tadić et al., 2015). Geographic information and the areas of cities in Henan Province were obtained from the National Earth System Science Data Centre (Science, 2015) and Henan Provincial Statistical Yearbooks, respectively.

2.4. Uncertainty analysis

2.4.1. Checking for random annual variations in the data

To exclude the possibility that the estimated results are due to random inter-annual variations, allowing the estimates to accurately reflect the changes resulting from the COVID-19 lockdown, we add an analysis of the changes in the emissions of each ammonia source in Henan Province from 2011 to 2018.

2.4.2. Comparison with previous studies

The estimated results of this study were compared with those of previous studies and used to analyse the variability of each ammonia source among regions with different industrial structures to ensure the accuracy of the estimation results.

2.4.3. Monte Carlo simulation

Quantitative analysis is highly important for emission inventories, which are used to analyse the uncertainty of each emission source, such that the inventory can provide effective help for future environmental protection and policy resolutions. Based on domestic and international research results (Streets et al., 2003; Wang et al., 2018a), we estimated the range of NH_3 emissions by using Monte Carlo simulation under the assumption that the input activity level data and emission factors followed a normal distribution. To ensure the accuracy of the simulation results, 10,000 Monte Carlo simulations with a 95 % confidence interval were performed to estimate the uncertainty in NH_3 emissions from each source.

3. Results and discussion

3.1. Anthropogenic NH_3 emission inventory

An anthropogenic NH_3 emission inventory for Henan Province in 2020 was established, based on the above study methods and activity levels, as shown in Table 1, and the contribution of different NH_3 emission sources to the total anthropogenic NH_3 emissions is shown in Fig. 2. Total NH_3 emissions were approximately 751.80 kt, comprising agricultural and non-agricultural sources of 634.10 kt and 117.69 kt, respectively, which accounts for 84.35 % and 18.60 % of the total emissions. Livestock waste management NH_3 emissions were the largest contribution from agricultural sources, accounting for 53.5 %, followed by farmland ecosystems at 30.9 %. Owing to the fact that Henan Province is a large agricultural province mainly focused on livestock and farming, its total production of pigs, cattle, sheep and poultry meat in 2020 was 5.441 million tonnes, the third largest in China, and the area of grain fields sown was 10,738.80 thousand hectares, accounting for approximately 9.2 % of the total area sown with grain crops in China (NBS, 2021). Compared with non-agricultural sources, livestock waste management has a larger breeding population, greater emission factors and longer breeding cycles. In addition, agricultural ecosystems in Henan Province are largely based on growing wheat and maize, which require much nitrogen fertiliser to provide nutrients; thus, more NH_3 emissions originate from agricultural sources. Among non-agricultural sources, biomass burning, human being and fuel combustion sources produce the most emissions, at 44.07 kt, 40.43 kt and 12.71 kt, respectively. These sources are associated with the burning of large amounts of straw fuelwood, a large rural population base and

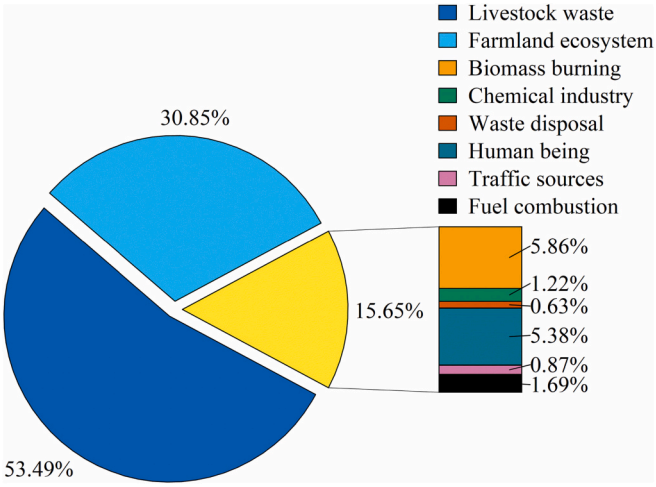

Fig. 2. Contribution of different NH_3 emission sources to total anthropogenic NH_3 emissions in 2020.

population consumption. At the urban level, Zhengzhou, as the capital city of Henan Province, has the highest NH_3 emissions from waste disposal, traffic and fuel combustion sources, which is closely related to being ranked number one in the province in terms of Gross Domestic Product (GDP) and urbanisation rate (HNBSB, 2021).

3.2. Changes in ammonia emissions

Differences in NH_3 emissions from 2019 to 2020 for a variety of sources are shown in Fig. 3. Total NH_3 emissions in 2020 were reduced by approximately 4 % compared with pre-COVID 2019 (NH_3 emissions in 2019 are shown in Table S11). The largest decrease was in traffic sources, from 9.72 kt to 6.55 kt at approximately 33 %, owing to the COVID-19 lockdown severely affecting the annual average mileage of private cars and minibuses (Li et al., 2020; Verma and Prakash, 2020). Livestock waste decreased by 15.52 kt, approximately 3.72 %, owing to road closures and shortages in feed supply to some farms and resulting in a decrease in the amount of food fed to livestock (Cao et al., 2020; Hafez and Attia, 2020). Nitrogen fertiliser application was slightly affected by the lockdown; however, owing to the short-term nature of the lockdown, fertilisation applications continued to be performed. Therefore there

Table 1
NH_3 emission inventory from different urban sources.

Cities	Agricultural sources		Non-agricultural sources						Total regional emissions kt
	Livestock waste kt	Farmland ecosystem kt	Biomass burning kt	Chemical industry kt	Waste disposal kt	Human being kt	Traffic sources kt	Fuel combustion kt	
Zhengzhou	6.97	6.07	1.30	0.23	1.42	2.49	1.42	2.64	22.54
Kaifeng	28.84	13.70	2.34	0.56	0.23	2.12	0.25	0.50	48.54
Luoyang	16.40	10.40	2.01	0.32	0.38	2.25	0.47	1.28	33.51
Pingdingshan	18.36	8.77	1.92	0.45	0.18	2.13	0.26	0.62	32.67
Anyang	15.81	11.34	2.39	0.56	0.18	2.35	0.38	0.56	33.57
Hebi	9.83	2.98	0.65	0.11	0.12	0.56	0.13	0.31	14.68
Xinxiang	20.59	13.89	2.70	0.79	0.28	2.43	0.46	0.75	41.88
Jiaozuo	8.24	5.56	1.13	0.24	0.19	1.19	0.29	0.50	17.32
Puyang	26.44	8.16	1.69	0.44	0.19	1.71	0.31	0.32	39.27
Xuchang	13.81	9.09	1.69	0.25	0.19	1.85	0.28	1.01	28.17
Luohe	12.88	5.81	0.98	0.16	0.20	0.98	0.17	0.37	21.56
Sanmenxia	7.45	4.04	0.71	0.10	0.09	0.79	0.13	0.38	13.70
Nanyang	48.11	31.92	5.56	1.09	0.30	4.39	0.45	0.70	92.51
Shangqiu	47.61	22.81	4.51	0.69	0.22	3.84	0.50	0.62	80.79
Xinyang	26.22	18.83	3.66	1.05	0.22	2.84	0.25	0.56	53.62
Zhoukou	48.84	28.93	5.43	1.36	0.11	4.73	0.43	0.75	90.57
Zhumadian	43.71	28.82	5.24	0.72	0.17	3.58	0.30	0.61	83.16
Jiyuan	2.03	0.85	0.18	0.04	0.10	0.22	0.08	0.23	3.73
Total emission sources kt	402.15 634.10	231.96	44.07 117.69	9.16	4.77	40.43	6.55	12.71	751.80

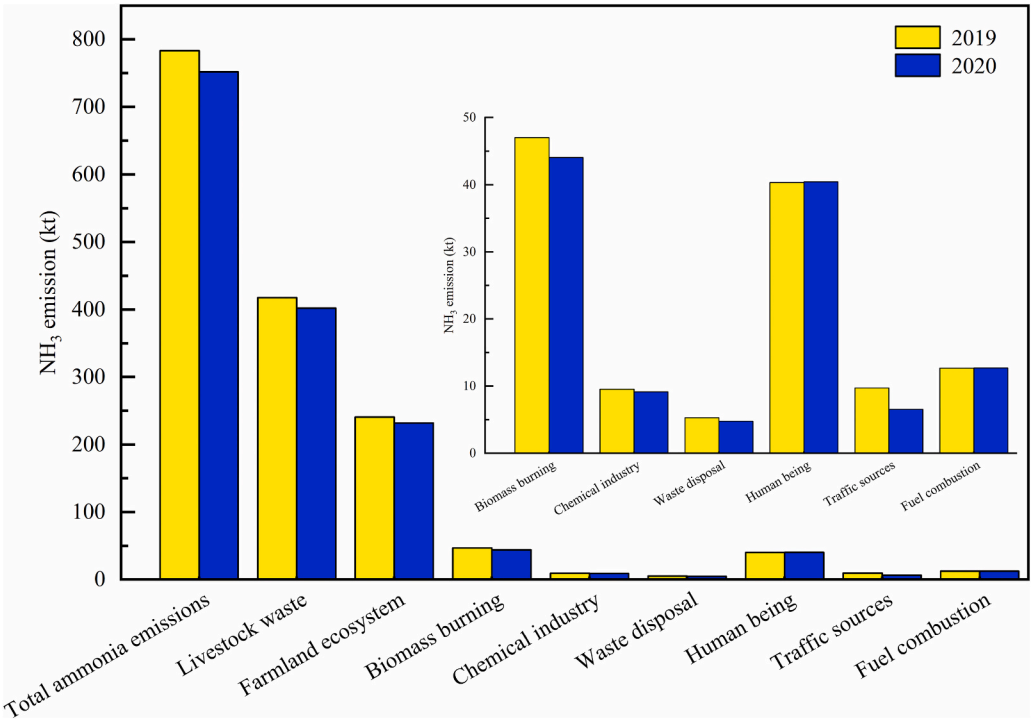

Fig. 3. NH_3 emissions from various sources in Henan Province from 2019 to 2020.

were no significant NH_3 changes in emissions. Biomass burning NH_3 emissions were reduced, and owing to the increased popularisation of natural gas, most rural villages used the wood-fired boiler once a day on average, greatly reducing the use of household fuelwood and straw. Waste disposal and chemical industry NH_3 emissions decreased by 0.53 kt and 0.39 kt, respectively, owing to the reduced operation of some waste disposal stations and plants (Filonchyk and Peterson, 2020). Contrary to the above-mentioned emission sources, human being emissions increased by 0.10 kt, owing to the increased use of dry latrines in rural areas as rural workers failed to return to urban work during the Spring Festival lockdown (Li et al., 2020). Fuel combustion also showed an increasing trend, by approximately 0.03 kt, owing to the reduction in outside gatherings and increased use of fuel as people stayed home (Du et al., 2021). There is an uncertainty in the discussion. In terms of time span, the previous study was based on a period of one to four months during the COVID-19 pandemic; however, considering that the span of the NH_3 emission inventory is typically a year and the epidemic did not cease during 2020, the changes in NH_3 emissions reflected this phenomenon to some extent in this study.

3.3. Livestock waste management analysis

Ammonia volatilisation reduces the N content of faeces, which affects the fertilisation efficiency and causes soil acidification and

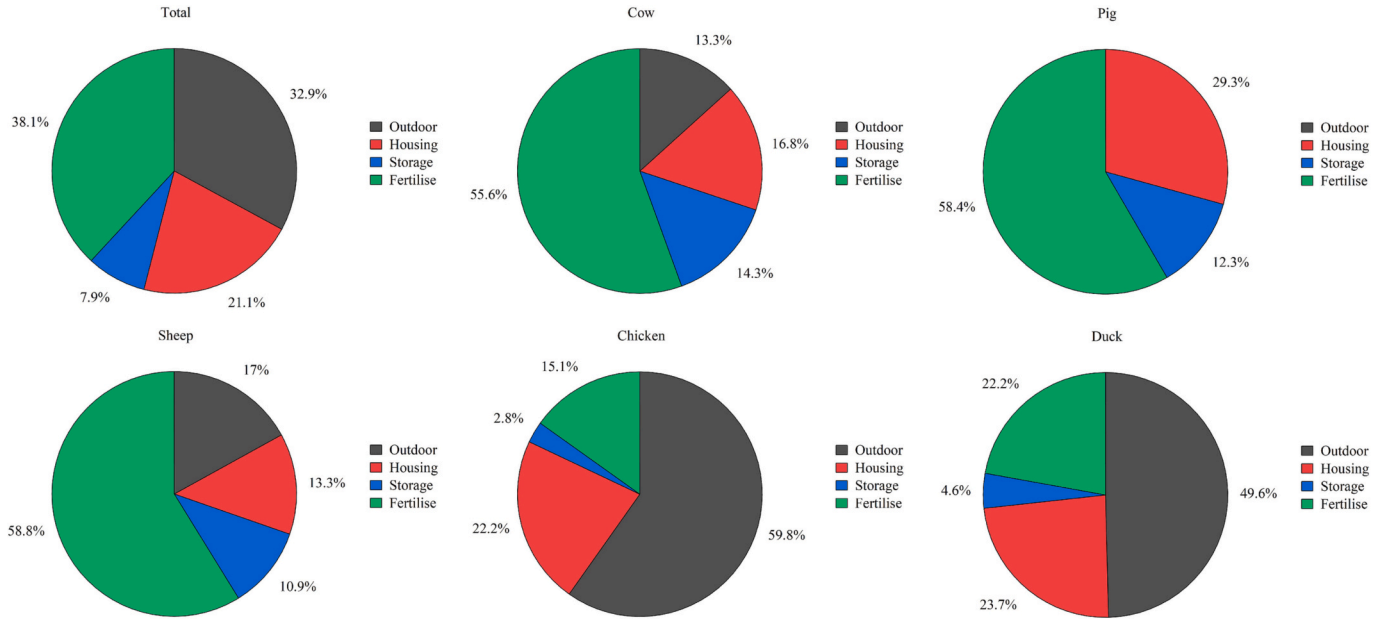

Fig. 4. Percentage of NH_3 emissions from different livestock at each stage.

problems in the eutrophication environment (Van der Stelt et al., 2007). As livestock waste was the primary emissions source, further analysis of livestock waste was conducted. To better provide targeted NH_3 emissions reduction measures for livestock breeding sources, this study classified livestock NH_3 emissions into four detailed stages: outdoor, housing, faeces storage and treatment and subsequent fertilisation. The percentage of NH_3 emissions for each stage is shown in Fig. 4. The faeces used in the fertilisation stage released the most NH_3 out of all the stages for all livestock except for chickens and ducks, accounting for 38.1 % of the total NH_3 for all stages. Ammonia volatilisation was affected by various factors such as wind speed, temperature, soil and rainfall in the faeces application phase. For instance, evening application reduces ammonia volatilisation by approximately 30 % compared to the early morning application (Gordon et al., 2001), with lower temperatures being the major reason in the evening. NH_3 losses can be decreased if fertiliser is applied during rain, as rain allows NH_3 from the soil surface to penetrate into the ground (Malgeryd, 1998), or by irrigating after fertiliser application. Deep burial of the soil decreases NH_3 losses further than surface spreading, by approximately 42 % (Huijsmans and de Mol, 1999). If a variety of conditions such as weather temperature, rainfall and soil are simultaneously considered, NH_3 losses can be significantly reduced (Smith et al., 2009). There are also measures that can be taken to reduce NH_3 losses during the NH_3 faeces management phase, including the outdoor, housing, faeces storage and faeces treatment phases, in which the faeces pass through a pre-management phase to be ultimately used for fertiliser application. Chickens and ducks release more NH_3 while in the outdoors; therefore, outdoor faeces should be transferred in time, or the soil should be covered on the faeces to reduce the loss of NH_3. In addition, NH_3 volatilisation can be decreased by mixing chemicals into the manure. For example, the addition of phosphoric acid or alum decreases NH_3 by 44 % and 62 %, respectively (Delaune et al., 2004). The percentages of NH_3 emissions from various livestock categories to the total NH_3 emissions from livestock farming are shown in Fig. S1. Laying hens, goats and pigs were the top three largest types of NH_3 emissions, with emissions of 131.48 kt, 69.74 kt and 64.97 kt, accounting for 32.69 %, 17.34 % and 16.16 % of the total NH_3 emissions, respectively. Laying hens accounted for the largest proportion of NH_3 emissions, owing to the high demand for eggs and egg products in human daily lives. Goats and meat pigs accounted for a larger proportion of the livestock population, owing to the high level of rearing and, thus, higher NH_3 emission factors. The contribution of dairy cows, sows and sheep was lower, owing to low farming numbers. Also affected by road closures (Hafez and Attia, 2020), feed supplies on farms were reduced, resulting in decreased NH_3 emissions.

3.4. N fertiliser NH_3 emissions in different cities

Farmland ecosystems were the second largest emission source in Henan Province, of which N fertiliser application of NH_3 emissions amounted to 209.78 kt, accounting for 90.44 % of the total emissions from farmland ecosystem. Therefore, NH_3 emissions from N fertiliser application were further analysed in this study. Fig. 5 shows the contribution from N fertiliser application to NH_3 emissions in each urban area. Nanyang, Zhoukou and Zhumadian were the top three cities in NH_3 emissions, which were 28.76 kt, 26.23 kt and 25.87 kt, respectively, mainly related to the sown area of crops. The sown areas were 2020.56, 1842.62 and 1816.93 thousand hectares (NBS, 2021), ranking as the top three largest areas in Henan Province. Meanwhile, the N fertiliser was mainly urea in each region, accounting for 81.77 % of the total emissions from N fertiliser application sources. The fertiliser was mostly spread; therefore, more NH_3 was volatilised during the application process. Zhoukou City had the highest NH_3 emission intensity at 2.19 t km^{-2}. Sanmenxia City has the lowest NH_3 emission intensity at 0.35 t km^{-2}. To a certain extent, the NH_3 emission intensity of N fertiliser reflected the pollution level of NH_3 production when N fertiliser was applied in each city. NH_3 losses during N fertiliser application were affected by the same conditions as faeces application such as weather temperature, soil and precipitation, mentioned in the faeces application discussion above. New high-efficiency urea can replace traditional urea, using high N fertiliser and organic fertiliser instead of chemical fertiliser to reduce NH_3 losses and improve yield and resource utilisation (Yang et al., 2019). Improved fertilisers are being used, such as NBPT (N-(n-butyl) phosphorothioic triamide) added to UAN (urea ammonium nitrate solution) fertiliser, which reduces NH_3 emissions by 50 % (Klimczyk et al., 2021). Reducing unnecessary fertiliser application and using high-protein animal feed can provide up to 30 % of the NH_3 reduction potential without increasing abatement costs or reducing agricultural productivity (Zhang et al., 2020). Meanwhile, enhancing agricultural production, updating technologies in a timely fashion and taking measures to control NH_3 production in livestock waste and N fertiliser application can be the path towards gradually achieving agricultural NH_3 reduction.

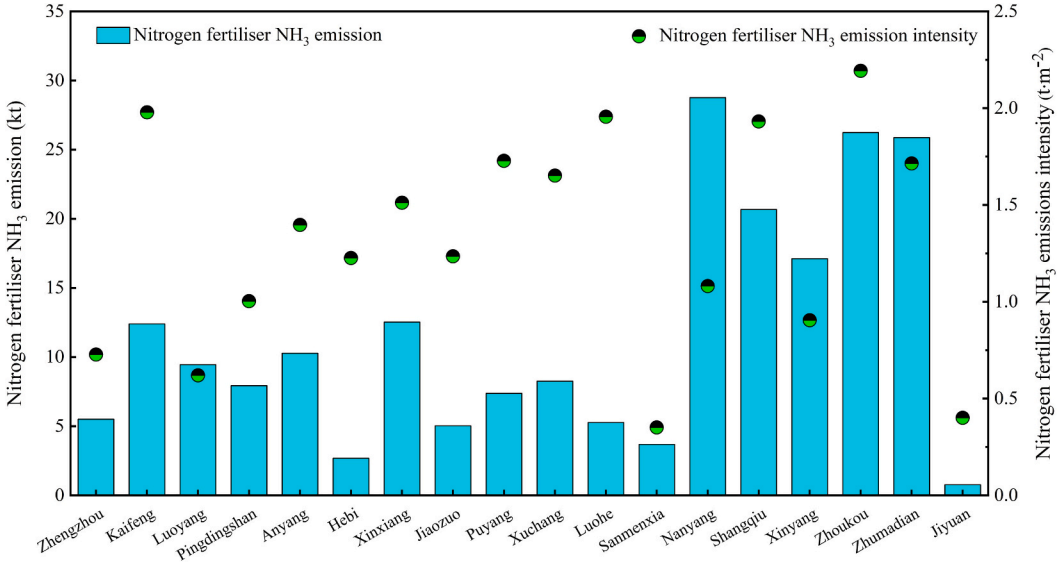

Fig. 5. N fertiliser NH_3 emissions and intensity in different cities.

3.5. Spatial distribution characteristics

ArcGIS was used to obtain information regarding the geographic boundaries of Henan Province to map the spatial distribution and intensity of NH_3 emissions in Henan Province in 2020. NH_3 emissions were characterised by a clear hierarchical distribution in space. As can be seen in Fig. 6a (left), there was a gradual increase in NH_3 emissions from north-west to south-east in Henan Province. NH_3 emissions were low in the north-west, such as the cities of Sanmenxia, Jiyuan and Jiaozuo, of which Jiyuan exhibited the smallest emissions at 3.73 kt. NH_3 emissions were high in the south-eastern part, for example in Nanyang City, Zhoukou City and Shangqiu City, of which Nanyang City had the largest emissions at 92.51 kt, accounting for 12.31 % of NH_3 emissions in the entire Henan Province. The above distribution of NH_3 emissions is mainly related to the area of crops sown and livestock produced in each city, starting from the north-west to the south-east from which the level of agricultural activity gradually increased; thus, the above changes occurred. As can be seen in Fig. 6(b) (right), the intensity of NH_3 emissions gradually increased from west to east. The emission intensity was low in Sanmenxia, Luoyang and Jiaozuo, of which Sanmenxia had the lowest intensity at 1.31 t km^{-2}. The emission intensity was high in Puyang, Luohe and Kaifeng, of which Puyang exhibited the highest intensity, at 9.19 t km^{-2}. The intensity of NH_3 emissions is mainly determined by a combination of urban area and level of agricultural activity.

3.6. Checking for random annual variations in the data

There is a large magnitude of random variation that occurs annually in the area of forest fires in the biomass burning ammonia emission sources. For instance, the area of forest fires in 2014 was 33,400,000 m^2 and 30,000 m^2 in 2015, corresponding to NH_3 emissions of 32.88 kt and 0.25 kt, respectively. This led to random variations in the trend of total NH_3 emissions, preventing a reliable analysis of the variations. We have placed the trends of biomass burning in the supplementary material Fig. S2, and the trends of total NH_3 emissions excluding biomass burning and other sources of NH_3 emissions are shown in Fig. 7 (right b is an unfolding of some sources from left a). Total NH_3 emissions fluctuated before 2015 and began to decrease steadily after 2015, with the largest decrease occurring in 2020. Livestock waste management gradually increased before 2015 and significantly decreased by 2016. Then, it gradually increased after 2016 and was decreasing by 2020. The farmland ecosystem has not changed significantly, maintaining a steady decrease. Human being and fuel combustion decreased gradually from 2011 to 2019 and increased slightly in 2020. Chemical industry maintained a steady decrease from 2012. Waste disposal kept increasing steadily from 2011 to 2019 and decreased slightly in 2020. Traffic sources kept a steady increase from 2011 to 2019 and decreased significantly in 2020. The above changes show that the ammonia emission sources more significantly changed by the COVID-19 epidemic lockdown were waste disposal, fuel combustion, human being, biomass burning, traffic sources and livestock waste management, and the most insignificant changes were in chemical industry and farmland ecosystem.

3.7. Comparison with previous studies

As Fig. 3 shows, the total NH_3 emissions during the 2020 COVID-19 lockdown were approximately 4 % lower than in 2019, before the lockdown. Considering that the total NH_3 emissions were slightly affected by the lockdown, this study remains comparable to NH_3 emission inventory studies performed before the onset of COVID-19, with the results shown in Table S13. Livestock waste and nitrogen fertiliser application both significantly contributed to NH_3 emissions in different provinces, with the sum of their contributions ranging from 55.19 % to 95.60 %. Compared with the NH_3 emissions of Jiangsu Province in 2017 estimated by Hou et al. (2019), Guangdong Province in 2010 estimated by Shen et al. (2014) and Zhejiang Province in 2017 estimated by Zhao et al. (2020), this study showed high emissions, mainly due to the different industrial structures of the provinces. Henan Province is one of the largest agricultural provinces in China, whose total grain production approaches one-tenth of the national total, and its cattle, pig and poultry rearing and poultry, egg and meat production rank among the top four in the country. Jiangsu Province has the largest manufacturing cluster and the highest GDP per capita continuously since 2019, ranking it as one of the most economically active provinces in China. Guangdong Province has ranked at the top in GDP in China continuously since 1989 as China's largest economic province and representing 1/8 of the total economic output of the country. Zhejiang Province contains abundant marine resources and a wide variety of organisms, renowned as the 'fish warehouse of China', with a coastline of total length 6486.24 km, 20.3 % of the total coastline in China and ranked first in China. Compared with the NH_3 emissions estimated by Zhou et al. (2021) for Shandong Province in 2017 and Feng et al. (2015) for Sichuan Province in 2012, the NH_3 emissions estimated results in this study are lower, mainly due to the variability in activity levels and crop cultivation structures among the large agricultural provinces. Shandong Province had the highest rate of arable land and is China's largest agricultural province, consistently leading all provinces in China in terms of value added in agriculture. Sichuan Province was also a major agricultural province with a tradition

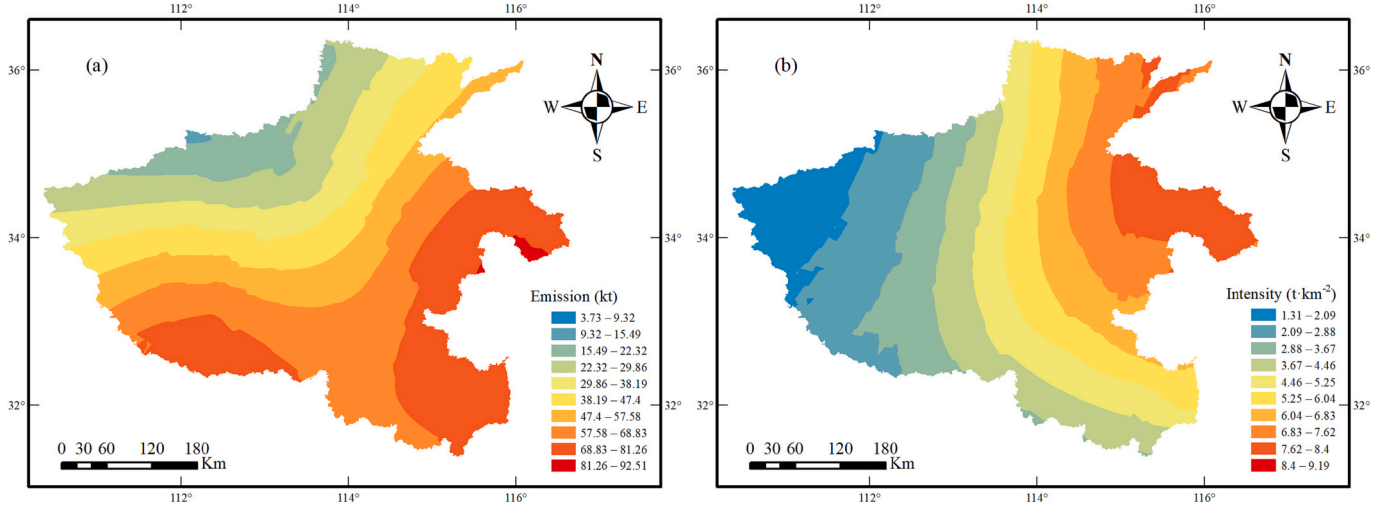

Fig. 6. NH_3 emissions and intensity of each prefecture-level city in Henan Province in 2020.

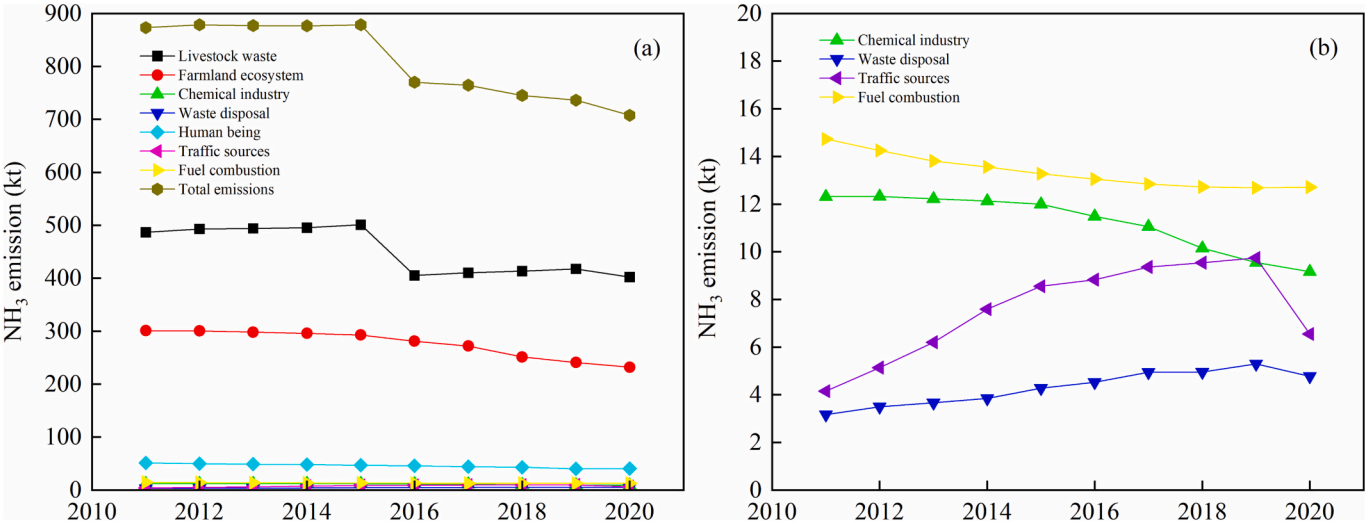

Fig. 7. Analysis of the change trend of each source from 2011 to 2020.

of intensive farming and a three-season per year farming system. Among the food crops, rice, wheat and corn have clear species advantages, especially rice, whose yield contributes over 40 % of the total grain production. Compared with the study of Henan Province by Wang et al. (2018b), these results are lower. First, the Wang et al. study considered a certain time span, and the NH_3 emission factors, NH_3 emission reduction measures and efficiencies adopted by various emission sources at that time were different. Furthermore, this study does not account for livestock with lower breeding numbers, such as donkeys and mules, for which there was some variability in activity level data (information sources for various regions are shown in Table S10).

3.8. Monte Carlo simulation

Uncertainty in the NH_3 emission inventory is mainly due to the lack of activity level data and choice of emission factors. The uncertainties of the different sources are shown in Table S14. Uncertainty was higher in the traffic sources and chemical industry, at [−25.34 %, 25.66 %] and [−24.09 %, 23.93 %], respectively. Based on the months affected by the 2020 COVID-19 lockdown, the annual average distance travelled by both private cars and minibuses from traffic sources decreased to some extent and differed from the actual distance travelled. The production of some chemical industries was affected by COVID-19, and the collected data deviated from the actual situation. Uncertainty is low for human being and biomass burning as the activity level data for human beingemissions were based on rural population figures from the statistical yearbook, and the activity level data of household straw and household firewood in biomass burning were obtained from rural visits and surveys, resulting in low uncertainty. Farmed donkeys, horses and mules were not included in the livestock waste farming calculations owing to their small numbers. Nevertheless, the breeding considered in the calculation was categorised into three methods: free-range, intensive and grazing. Meanwhile, the calculation of excrement and urine NH_3 emissions was classified into four stages: outdoor, housing, manure storage and treatment and subsequent fertilisation. The data and factors were taken from the statistical yearbooks and guidelines; thus, the uncertainty was low. In calculating the N fertiliser application, the average temperature of Henan Province was considered to be the annual temperature. Soil pH was calculated by considering its soil acidity and alkalinity ratio, which has some uncertainty. However, N fertilisers were calculated on a species basis, reducing the uncertainty in NH_3 emissions. Uncertainties in waste disposal and fuel combustion emission sources were mainly derived from the choice of emission factors, and the reference standards were based on the selection of materials. The total NH_3 emissions estimated in this study were 671.65 kt to 851.94 kt, and the uncertainty range was [−10.66 %,13.32 %]. Therefore, this NH_3 emission inventory generally contained high accuracy (information of Monte Carlo simulation is shown in Table S9).

3.9. Impact of ammonia on haze pollution and reduction in emissions

As shown in Fig. 3, our estimates show that the total NH_3 emissions are only reduced by approximately 4 %, a slight reduction compared to emissions of SO_2 and NO_x. Zheng et al. (2021) showed that SO_2 and NO_x during the lockdown were reduced by 27 % and 36 %, respectively, and Bao and Zhang (2020) also confirmed the significant reduction in SO_2 and NO_x, revealing that ammonia was enriched during the lockdown period. Previous studies have shown that under conditions of high atmospheric ammonia concentration, SO_2 and NO_x are rapidly oxidised to form particulate matter (Jiang and Xia, 2017), causing severe haze events. Huang et al. (2021) indicated that the enhanced formation of secondary particulate matter aggravated the haze pollution during the COVID-19 lockdown. Therefore, to alleviate haze in China, the focus should be on reducing NH_3 emissions compared to air pollutants such as SO_2 and NO_x. Numerous previous studies have shown that SNA (SO_4^{2-}, NO_3^- and NH_4^+) concentrations can be significantly reduced only when NH_3 is reduced compared to SO_2 and NO_x emissions (Erisman and Schaap, 2004). $PM_{2.5}$ can be reduced by more than 30 % if levels of NH_3 and NO_x emissions are reduced simultaneously (Bauer et al., 2016). Ti et al. (2022) showed that agricultural ammonia in China could be reduced by 74 % if highly efficient reduction techniques were applied in combination, and it is possible to reduce $PM_{2.5}$ pollution from 43 to 28 μg m^{-3}. Some researchers believe that NH_3 reduction can be more effective in mitigating $PM_{2.5}$ pollution based on low-cost consumption than the reduction of air pollutants such as SO_2 and NO_x (Gu et al., 2021; Pinder et al., 2007; Wu et al., 2016). Ammonia reduction is also a useful complement to SO_2 and NO_x emission reduction, reducing the cost of air pollutant reduction and achieving the goal of air quality improvement. Therefore, refining ammonia reduction is very crucial for alleviating haze pollution. As can be seen in Fig. 7, NH_3 emissions from the farmland ecosystem are steadily reducing annually, which is due to improved technology mitigating ammonia from nitrogen fertilisation. Traffic sources, although rising until 2020, should decrease in the future with the rise of new energy vehicles (He et al., 2020). Human and fuel combustion NH_3 emissions will keep decreasing in the future as urbanisation rates and natural gas penetration increase. Unfortunately, ammonia reductions are urgent, and we have learned that ammonia reductions take place very slowly. Meanwhile, livestock waste

management NH_3 emission sources, which account for 51 %–55 % of the total anthropogenic sources (percentage as shown in Fig. S3), may continue to rise after the close of the pandemic. Therefore, it is necessary to upgrade control measures and set specific targets for NH_3 emission reduction; only in this way can haze pollution be alleviated.

4. Conclusion

We established an anthropogenic NH_3 emission inventory for Henan Province during the 2020 COVID-19 lockdown based on detailed activity level data and accurate emission factors. Total NH_3 emissions were 751.80 kt, and agriculture was the major emission source in Henan Province with 87.07 % of the total NH_3 emissions. Total NH_3 emissions were slightly affected by the COVID-19 lockdown, approximately 4 % lower than before the lockdown. The biggest reduction was in traffic sources, from 9.72 kt to 6.55 kt, reduced by approximately 33 %. Next, waste disposal and biomass burning were reduced by 9.97 % and 6.19 %, respectively. Human emissions and fuel combustion slightly increased. Livestock waste emissions only decreased by 3.72 %, and other agricultural emissions changed insignificantly. Non-agricultural sources were more severely influenced by the COVID-19 lockdown than agricultural sources.

Except for chickens and ducks, the release of NH_3 was highest in the fertilisation stage, accounting for 38.1 % of the total NH_3 emissions in each stage. The largest NH_3 emissions were from laying hens, 131.48 kt, accounting for 32.69 % of the total NH_3 emissions from livestock waste. N fertiliser application accounted for 90.44 % of the NH_3 emissions from farmland ecosystems, of which urea was the main N fertiliser and its NH_3 emissions accounted for 81.77 % of the NH_3 emissions from N fertiliser application. Compared with previous studies, agriculture tends to be the main source of emissions, and NH_3 emissions are higher in areas dominated by agriculture. Uncertainty analysis showed that the uncertainty range for total NH_3 emissions was [−10.66 %,13.32 %], with higher uncertainty for traffic sources and the chemical industry. The spatial distribution characteristics showed that NH_3 emissions in southeast Henan Province were higher, of which Nanyang City had the largest NH_3 emissions, 92.51 kt, accounting for 12.31 % of the total NH_3 emissions. The NH_3 emissions intensity gradually increased from west to east, from which Puyang City had the highest emissions intensity, 9.19 $t{\cdot}km^{-2}$.

Total NH_3 emissions were slightly affected during the COVID-19 lockdown, even though the level of human activity was very low. Owing to agriculture remaining the main source of NH_3 emissions during the lockdown, agriculture was only slightly affected, and productivity recovered more quickly after the lockdown was lifted. Thus, NH_3 emissions in Henan Province on the North China Plain remained high. Corresponding to severe haze days, NH_3 was one of the key factors in inducing haze. In the next study, an NH_3 emission inventory will be established on a larger scale to analyse the corresponding change relationship between NH_3 emission and $PM_{2.5}$ so as to enhance the accuracy and comprehensiveness of the discussion.

CRediT authorship contribution statement

Shili Yang, Mingya Wang, Wenju Wang: Investigation, Conceptualization, Writing, Formal analysis, Data Curation, Editing and Original Draft; Xuechun Zhang and Qiao Han: Investigation, Experimental analysis, Data Curation, Review; Haifeng Wang: Investigation and Experimental analysis. Qinqing Xiong and Chunhui Zhang: Experimental analysis and Data Curation; Mingshi Wang: Conceptualization, Methodology, Supervision, Project administration and Review.

Declaration of competing interest

No conflict of interest exists in the submission of this manuscript, and the manuscript is approved by all authors for publication.

Data availability

Data will be made available on request.

Acknowledgments

This work was supported by the National Natural Science Foundation of China (No.41977284).

Appendix A. Supplementary data

Supplementary data to this article can be found online at https://doi.org/10.1016/j.scitotenv.2023.166857.

References

Bao, R., Zhang, A., 2020. Does lockdown reduce air pollution? Evidence from 44 cities in northern China. Sci. Total Environ. 731, 139052 https://doi.org/10.1016/j.scitotenv.2020.139052.

Battye, W., Aneja, V.P., Roelle, P.A., 2003. Evaluation and improvement of ammonia emissions inventories. Atmos. Environ. 37 (27), 3873–3883. https://doi.org/10.1016/S1352-2310(03)00343-1.

Bauer, S.E., Tsigaridis, K., Miller, R., 2016. Significant atmospheric aerosol pollution caused by world food cultivation. Geophys. Res. Lett. 43 (10), 5394–5400.

Bouwman, A.F., Lee, D.S., Asman, W.A.H., Dentener, F.J., van der Hoek, K.W., Olivier, J. G.J., 1997. A global high-resolution emission inventory for ammonia. Glob. Biogeochem. Cycles 11 (4), 561–587. https://doi.org/10.1029/97GB02266.

Cao, L., Li, T., Wang, R., Zhu, J., 2020. Impact of covid-19 on China's agricultural trade. China Agric. Econ. Rev. 13 (1), 1–21. https://doi.org/10.1108/CAER-05-2020-0079.

Cao, Y., Bai, Z., Misselbrook, T., Wang, X., Ma, L., 2021. Ammonia emissions from different pig production scales and their temporal variations in the north China plain. J. Air Waste Manage. Assoc. 71 (1), 23–33. https://doi.org/10.1080/10962247.2020.1815895.

Chang, Y., Huang, R.J., Ge, X., Huang, X., Hu, J., Duan, Y., Zou, Z., Liu, X., Lehmann, M. F., 2020. Puzzling haze events in China during the coronavirus (covid-19) shutdown. Geophys. Res. Lett. 47 (12), n/a–n/a. https://doi.org/10.1029/2020GL088533.

Chen, S., Cheng, M., Guo, Z., Xu, W., Du, X., Li, Y., 2020. Enhanced atmospheric ammonia (nh3) pollution in China from 2008 to 2016: evidence from a combination of observations and emissions. Environ. Pollut. 263, 114421 https://doi.org/10.1016/j.envpol.2020.114421.

Dantas, G., Siciliano, B., França, B.B., Da Silva, C.M., Arbilla, G., 2020. The impact of covid-19 partial lockdown on the air quality of the city of Rio de Janeiro, Brazil. Sci. Total Environ. 729, 139085 https://doi.org/10.1016/j.scitotenv.2020.139085.

Delaune, P.B., Moore Jr., P.A., Daniel, T.C., Lemunyon, J.L., 2004. Effect of chemical and microbial amendments on ammonia volatilization from composting poultry litter. J. Environ. Qual. 33 (2), 728–734. https://doi.org/10.2134/jeq2004.0728.

Du, W., Wang, J., Wang, Z., Lei, Y., Huang, Y., Liu, S., Wu, C., Ge, S., Chen, Y., Bai, K., Wang, G., 2021. Influence of covid-19 lockdown overlapping chinese spring festival on household pm2.5 in rural chinese homes. Chemosphere 278, 130406. https://doi.org/10.1016/j.chemosphere.2021.130406.

Erisman, J.W., Schaap, M., 2004. The need for ammonia abatement with respect to secondary pm reductions in europe. Environ. Pollut. 129 (1), 159–163.

Farren, N.J., Davison, J., Rose, R.A., Wagner, R.L., Carslaw, D.C., 2020. Underestimated ammonia emissions from road vehicles. Environ. Sci. Technol. 54 (24), 15689–15697. https://doi.org/10.1021/acs.est.0c05839.

Feng, X., Wang, X., He, M., Han, L., 2015. A 2012-based anthropogenic ammonia emission inventory and its spatial distribution in Sichuan province. Acta Sci. Circumst. 35, 394–401 (In Chinese).

Filonchyk, M., Peterson, M., 2020. Air quality changes in Shanghai, China, and the surrounding urban agglomeration during the covid-19 lockdown. J. Geovisual. Spatial Analysis 4 (2), 1–7. https://doi.org/10.1007/s41651-020-00064-5.

Frey, H.C., Zheng, J., 2002. Quantification of variability and uncertainty in air pollutant emission inventories: method and case study for utility nox emissions. J. Air Waste Manage. Assoc. 52 (9), 1083–1095. https://doi.org/10.1080/10473289.2002.10470837.

Goebes, M.D., Strader, R., Davidson, C., 2003. An ammonia emission inventory for fertilizer application in the United States. Atmos. Environ. 37 (18), 2539–2550. https://doi.org/10.1016/S1352-2310(03)00129-8.

Gordon, R., Jamieson, R., Rodd, V., Patterson, G., Harz, T., 2001. Effects of surface manure application timing on ammonia volatilization. Can. J. Soil Sci. 81 (4), 525–533. https://doi.org/10.4141/s00-092.

Gu, B., Zhang, L., Van Dingenen, R., Vieno, M., Van Grinsven, H.J., Zhang, X., Zhang, S., Chen, Y., Wang, S., Ren, C., 2021. Abating ammonia is more cost-effective than nitrogen oxides for mitigating pm2. 5 air pollution. Science 374 (6568), 758–762.

Hafez, H.M., Attia, Y.A., 2020. Challenges to the poultry industry: current perspectives and strategic future after the covid-19 outbreak. Front. Vet. Sci. 7, 516. https://doi.org/10.3389/fvets.2020.00516.

He, L., Pei, L., Yang, Y., 2020. An optimised grey buffer operator for forecasting the production and sales of new energy vehicles in China. Sci. Total Environ. 704, 135321 https://doi.org/10.1016/j.scitotenv.2019.135321.

Hellsten, S., Dragosits, U., Place, C.J., Vieno, M., Dore, A.J., Misselbrook, T.H., Tang, Y. S., Sutton, M.A., 2008. Modelling the spatial distribution of ammonia emissions in the UK. Environ. Pollut. 154 (3), 370–379. https://doi.org/10.1016/j.envpol.2008.02.017.

HNBSB, 2021. Henan Statistical Yearbook 2021. Henan Provincial Bureau of Statistics.

Hou, X., Yu, X., Shen, L., Zhao, R., Wang, G., Zhang, Y., 2019. Establishment and characteristics of an artificial ammonia emissions inventory in Jiangsu province from 2013 to 2017. Huan Jing ke Xue= Huanjing Kexue 40 (11), 4862–4869 (In Chinese).

Hu, J., Wang, Y., Ying, Q., Zhang, H., 2014. Spatial and temporal variability of pm2. 5 and pm10 over the North China plain and the yangtze river delta, China. Atmos. Environ. 95, 598–609. https://doi.org/10.1016/j.atmosenv.2014.07.019.

Huang, C., Chen, C.H., Li, L., Cheng, Z., Wang, H.L., Huang, H.Y., Streets, D.G., Wang, Y. J., Zhang, G.F., Chen, Y.R., 2011. Emission inventory of anthropogenic air pollutants and voc species in the yangtze river delta region, China. Atmos. Chem. Phys. 11 (9), 4105–4120. https://doi.org/10.5194/acp-11-4105-2011.

Huang, X., Song, Y., Li, M., Li, J., Huo, Q., Cai, X., Zhu, T., Hu, M., Zhang, H., 2012. A high-resolution ammonia emission inventory in China. Glob. Biogeochem. Cycles 26 (1), B1030. https://doi.org/10.1029/2011GB004161.

Huang, X., Ding, A., Gao, J., Zheng, B., Zhou, D., Qi, X., Tang, R., Wang, J., Ren, C., Nie, W., 2021. Enhanced secondary pollution offset reduction of primary emissions during covid-19 lockdown in China. Natl. Sci. Rev. 8 (2), a137 https://doi.org/10.1093/nsr/nwaa137.

Huijsmans, J.F.M., de Mol, R.M., 1999. A model for ammonia volatilization after surface application and subsequent incorporation of manure on arable land. J. Agric. Eng. Res. 74 (1), 73–82. https://doi.org/10.1006/jaer.1999.0438.

Huo, Q., Cai, X., Kang, L., Zhang, H., Song, Y., Zhu, T., 2015. Estimating ammonia emissions from a winter wheat cropland in North China plain with field experiments and inverse dispersion modeling. Atmos. Environ. 104, 1–10. https://doi.org/10.1016/j.atmosenv.2015.01.003.

Jiang, B., Xia, D., 2017. Role identification of nh3 in atmospheric secondary new particle formation in haze occurrence of China. Atmos. Environ. 163, 107–117. https://doi.org/10.1016/j.atmosenv.2017.05.035.

Ju, X., Xing, G., Chen, X., Zhang, S., Zhang, L., Liu, X., Cui, Z., Yin, B., Christie, P., Zhu, Z., 2009. Reducing environmental risk by improving n management in intensive chinese agricultural systems. Proc. Natl. Acad. Sci. 106 (9), 3041–3046. https://doi.org/10.1073/pnas.0813417106.

Kang, Y., Liu, M., Song, Y., Huang, X., Yao, H., Cai, X., Zhang, H., Kang, L., Liu, X., Yan, X., 2016. High-resolution ammonia emissions inventories in China from 1980 to 2012. Atmos. Chem. Phys. 16 (4), 2043–2058. https://doi.org/10.5194/acp-16-2043-2016.

Kerimray, A., Baimatova, N., Ibragimova, O.P., Bukenov, B., Kenessov, B., Plotitsyn, P., Karaca, F., 2020. Assessing air quality changes in large cities during covid-19 lockdowns: the impacts of traffic-free urban conditions in Almaty, Kazakhstan. Sci. Total Environ. 730, 139179 https://doi.org/10.1016/j.scitotenv.2020.139179.

Klimczyk, M., Siczek, A., Schimmelpfennig, L., 2021. Improving the efficiency of urea-based fertilization leading to reduction in ammonia emission. Sci. Total Environ. 771, 145483 https://doi.org/10.1016/j.scitotenv.2021.145483.

Krupa, S.V., 2003. Effects of atmospheric ammonia (nh3) on terrestrial vegetation: a review. Environ. Pollut. 124 (2), 179–221. https://doi.org/10.1016/S0269-7491(02)00434-7.

Li, L., Li, Q., Huang, L., Wang, Q., Zhu, A., Xu, J., Liu, Z., Li, H., Shi, L., Li, R., Azari, M., Wang, Y., Zhang, X., Liu, Z., Zhu, Y., Zhang, K., Xue, S., Ooi, M.C.G., Zhang, D., Chan, A., 2020. Air quality changes during the covid-19 lockdown over the yangtze river delta region: an insight into the impact of human activity pattern changes on air pollution variation. Sci. Total Environ. 732, 139282 https://doi.org/10.1016/j.scitotenv.2020.139282.

Li, M., Wang, T., Xie, M., Li, S., Zhuang, B., Fu, Q., Zhao, M., Wu, H., Liu, J., Saikawa, E., Liao, K., 2021. Drivers for the poor air quality conditions in North China plain during the covid-19 outbreak. Atmos. Environ. 246, 118103 https://doi.org/10.1016/j.atmosenv.2020.118103.

Małgeryd, J., 1998. Technical measures to reduce ammonia losses after spreading of animal manure. Nutr. Cycl. Agroecosyst. 51 (1), 51–57. https://doi.org/10.1023/A:1009751210447.

MEP, 2014a. Technical Guidelines for Preparation of Atmospheric Ammonia Emission Inventory (for Trial Implementation). Ministry of Ecology and Environment of the People's Republic of China, pp. 8–19.

MEP, 2014b. Technical Guidelines for the Development of Air Pollutant Emission Inventories for Biomass Combustion Sources (for Trial Implementation). Ministry of Ecology and Environment of the People's Republic of China.

MEP, 2014c. Technical Guide for Compilation of Road Motor Vehicle Emission Inventory (Trial). Ministry of Ecology and Environment of the People's Republic of China.

MOF, 2011. The Notice on Issuing the Implementation Plan for Comprehensive Utilization of Crop Straw in the 12th Five-year Plan. Ministry of Finance People's Republic of China.

NBS, 2021. China Statistical Yearbook 2021. National Bureau of Statistics of China.

NESSDC, 2015. Administrative Divisions in Henan Province. National Earth System Science Data Center.

Olivier, J.G.J., Bouwman, A.F., Van der Hoek, K.W., Berdowski, J.J.M., 1998. Global air emission inventories for anthropogenic sources of nox, nh3 and n2o in 1990. Environ. Pollut. 102 (1, Supplement 1), 135–148. https://doi.org/10.1016/S0269-7491(98)80026-2.

Pain, B.F., Van der Weerden, T.J., Chambers, B.J., Phillips, V.R., Jarvis, S.C., 1998. A new inventory for ammonia emissions from U.K. Agric. Atmos. Environ. 32 (3), 309–313. https://doi.org/10.1016/S1352-2310(96)00352-4.

Pan, Y., Tian, S., Liu, D., Fang, Y., Zhu, X., Gao, M., Wentworth, G.R., Michalski, G., Huang, X., Wang, Y., 2018. Source apportionment of aerosol ammonium in an ammonia-rich atmosphere: an isotopic study of summer clean and hazy days in urban Beijing. J. Geophys. Res. Atmos. 123 (10), 5681–5689. https://doi.org/10.1029/2017JD028095.

Peng, J., Hu, M., Shang, D., Wu, Z., Du, Z., Tan, T., Wang, Y., Zhang, F., Zhang, R., 2021. Explosive secondary aerosol formation during severe haze in the North China plain. Environ. Sci. Technol. 55 (4), 2189–2207. https://doi.org/10.1021/acs.est.0c07204.

Pinder, R.W., Adams, P.J., Pandis, S.N., 2007. Ammonia emission controls as a cost-effective strategy for reducing atmospheric particulate matter in the eastern United States. Environ. Sci. Technol. 41 (2), 380–386. https://doi.org/10.1021/es060379a.

Ren, C., Huang, X., Wang, Z., Sun, P., Chi, X., Ma, Y., Zhou, D., Huang, J., Xie, Y., Gao, J., Ding, A., 2021. Nonlinear response of nitrate to nox reduction in China during the covid-19 pandemic. Atmos. Environ. 264, 118715 https://doi.org/10.1016/j.atmosenv.2021.118715.

Sarwar, G., Corsi, R.L., Kinney, K.A., Banks, J.A., Torres, V.M., Schmidt, C., 2005. Measurements of ammonia emissions from oak and pine forests and development of a non-industrial ammonia emissions inventory in Texas. Atmos. Environ. 39 (37), 7137–7153. https://doi.org/10.1016/j.atmosenv.2005.08.016.

Sekar, A., Jasna, R.S., Binoy, B.V., Mohan, P., Kuttiparichel Varghese, G., 2023. Air quality change and public perception during the covid-19 lockdown in India. Gondwana Res. 114, 15–29. https://doi.org/10.1016/j.gr.2022.04.023.

Shen, X.L., Yin, S.S., Zheng, J.Y., Lu, Q., Zhong, L.J., 2014. Anthropogenic ammonia emission inventory and its mitigation potential in Guangdong province. Acta Sci. Circumst. 34 (1), 43–53 (In Chinese).

Smith, E., Gordon, R., Bourque, C., Campbell, A., Génermont, S., Rochette, P., Mkhabela, M., 2009. Simulated management effects on ammonia emissions from field applied manure. J. Environ. Manag. 90 (8), 2531–2536. https://doi.org/10.1016/j.jenvman.2009.01.012.

Song, X., Jia, J., Wu, F., Niu, H., Ma, Q., Guo, B., Shao, L., Zhang, D., 2022. Local emissions and secondary pollutants cause severe pm2. 5 elevation in urban air at the south edge of the North China plain: results from winter haze of 2017–2018 at a mega city. Sci. Total Environ. 802, 149630 https://doi.org/10.1016/j.scitotenv.2021.149630.

Streets, D.G., Bond, T.C., Carmichael, G.R., Fernandes, S.D., Fu, Q., He, D., Klimont, Z., Nelson, S.M., Tsai, N.Y., Wang, M.Q., 2003. An inventory of gaseous and primary aerosol emissions in asia in the year 2000. J. Geophys. Res. Atmos. 108 (D21), 8809. https://doi.org/10.1029/2002JD003093.

Tadić, J.M., Ilić, V., Biraud, S., 2015. Examination of geostatistical and machine-learning techniques as interpolators in anisotropic atmospheric environments. Atmos. Environ. 111, 28–38. https://doi.org/10.1016/j.atmosenv.2015.03.063.

Ti, C., Han, X., Chang, S.X., Peng, L., Xia, L., Yan, X., 2022. Mitigation of agricultural nh3 emissions reduces pm2.5 pollution in China: a finer scale analysis. J. Clean. Prod. 350, 131507 https://doi.org/10.1016/j.jclepro.2022.131507.

Tian, H., Liu, Y., Li, Y., Wu, C., Chen, B., Kraemer, M.U., Li, B., Cai, J., Xu, B., Yang, Q., 2020. An investigation of transmission control measures during the first 50 days of the covid-19 epidemic in China. Science 368 (6491), 638–642. https://doi.org/10.1126/science.abb6105.

Timmer, B., Olthuis, W., Berg, A.V.D., 2005. Ammonia sensors and their applications—a review. Sensors Actuators B Chem. 107 (2), 666–677. https://doi.org/10.1016/j.snb.2004.11.054.

Van der Stelt, B., Temminghoff, E.J.M., Van Vliet, P.C.J., Van Riemsdijk, W.H., 2007. Volatilization of ammonia from manure as affected by manure additives, temperature and mixing. Bioresour. Technol. 98 (18), 3449–3455. https://doi.org/10.1016/j.biortech.2006.11.004.

Verma, A.K., Prakash, S., 2020. Impact of covid-19 on environment and society. J. Glob. Biosci. 9 (5), 7352–7363.

Wang, S., Nan, J., Shi, C., Fu, Q., Gao, S., Wang, D., Cui, H., Saiz-Lopez, A., Zhou, B., 2015. Atmospheric ammonia and its impacts on regional air quality over the megacity of Shanghai, China. Sci. Rep. UK 5 (1), 1–13. https://doi.org/10.1038/srep15842.

Wang, C., Yin, S., Bai, L., Zhang, X., Gu, X., Zhang, H., Lu, Q., Zhang, R., 2018a. High-resolution ammonia emission inventories with comprehensive analysis and evaluation in Henan, China, 2006–2016. Atmos. Environ. 193, 11–23. https://doi.org/10.1016/j.atmosenv.2018.08.063.

Wang, C., Yin, S., Yu, S., Wei, J., Gu, X., Gong, M., Zhang, R., 2018b. A 2013-based atmospheric ammonia emission inventory and its characteristic of spatial distribution in Henan province. Huan Jing ke Xue=Huanjing Kexue 39 (3), 1023–1030 (In Chinese).

Wang, C., Horby, P.W., Hayden, F.G., Gao, G.F., 2020. A novel coronavirus outbreak of global health concern. Lancet 395 (10223), 470–473. https://doi.org/10.1016/S0140-6736(20)30185-9.

Wang, W., Chen, C., Liu, D., Wang, M., Han, Q., Zhang, X., Feng, X., Sun, A., Mao, P., Xiong, Q., Zhang, C., 2022. Health risk assessment of pm2.5 heavy metals in county units of northern China based on Monte Carlo simulation and apcs-mlr. Sci. Total Environ. 843, 156777 https://doi.org/10.1016/j.scitotenv.2022.156777.

Webb, J., Misselbrook, T.H., 2004. A mass-flow model of ammonia emissions from Uk livestock production. Atmos. Environ. 38 (14), 2163–2176. https://doi.org/10.1016/j.atmosenv.2004.01.023.

Wu, Y., Gu, B., Erisman, J.W., Reis, S., Fang, Y., Lu, X., Zhang, X., 2016. Pm2.5 pollution is substantially affected by ammonia emissions in China. Environ. Pollut. 218, 86–94. https://doi.org/10.1016/j.envpol.2016.08.027.

Xu, W., Wu, Q., Liu, X., Tang, A., Dore, A.J., Heal, M.R., 2016. Characteristics of ammonia, acid gases, and pm2. 5 for three typical land-use types in the North China plain. Environ. Sci. Pollut. R. 23 (2), 1158–1172. https://doi.org/10.1007/s11356-015-5648-3.

Yang, F., Tan, J., Zhao, Q., Du, Z., He, K., Ma, Y., Duan, F., Chen, G., 2011. Characteristics of pm 2.5 speciation in representative megacities and across China. Atmos. Chem. Phys. 11 (11), 5207–5219.

Yang, Q., Liu, P., Dong, S., Zhang, J., Zhao, B., 2019. Effects of fertilizer type and rate on summer maize grain yield and ammonia volatilization loss in northern China. J. Soils Sediments 19 (5), 2200–2211. https://doi.org/10.1007/s11368-019-02254-1.

Yang, J., Wang, S., Zhang, R., Yin, S., 2022. Elevated particle acidity enhanced the sulfate formation during the covid-19 pandemic in Zhengzhou, China. Environ. Pollut. 296, 118716 https://doi.org/10.1016/j.envpol.2021.118716.

Yu, X., Shen, L., Hou, X., Yuan, L., Pan, Y., An, J., Yan, S., 2020. High-resolution anthropogenic ammonia emission inventory for the Yangtze river delta, China. Chemosphere 251, 126342. https://doi.org/10.1016/j.chemosphere.2020.126342.

Zhang, Y., Dore, A.J., Ma, L., Liu, X.J., Ma, W.Q., Cape, J.N., Zhang, F.S., 2010a. Agricultural ammonia emissions inventory and spatial distribution in the North China plain. Environ. Pollut. 158 (2), 490–501. https://doi.org/10.1016/j.envpol.2009.08.033.

Zhang, D.Q., Tan, S.K., Gersberg, R.M., 2010b. Municipal solid waste management in China: status, problems and challenges. J. Environ. Manag. 91 (8), 1623–1633. https://doi.org/10.1016/j.jenvman.2010.03.012.

Zhang, Y., Luan, S., Chen, L., Shao, M., 2011. Estimating the volatilization of ammonia from synthetic nitrogenous fertilizers used in China. J. Environ. Manag. 92 (3), 480–493. https://doi.org/10.1016/j.jenvman.2010.09.018.

Zhang, L., Chen, Y., Zhao, Y., Henze, D.K., Zhu, L., Song, Y., Paulot, F., Liu, X., Pan, Y., Lin, Y., 2018. Agricultural ammonia emissions in China: reconciling bottom-up and top-down estimates. Atmos. Chem. Phys. 18 (1), 339–355. https://doi.org/10.5194/acp-18-339-2018.

Zhang, X., Gu, B., van Grinsven, H., Lam, S.K., Liang, X., Bai, M., Chen, D., 2020. Societal benefits of halving agricultural ammonia emissions in China far exceed the abatement costs. Nat. Commun. 11 (1), 1–10. https://doi.org/10.1038/s41467-020-18196-z.

Zhao, D.W., Wang, A.P., 1994. Estimation of anthropogenic ammonia emissions in asia. Atmos. Environ. 28 (4), 689–694. https://doi.org/10.1016/1352-2310(94)90045-0.

Zhao, R., Yu, X., Hou, X., Shen, L., 2020. Establishment and spatial distribution of anthropogenic ammonia emission inventory in Zhejiang province. Huan Jing ke Xue=Huanjing Kexue 41 (9), 3976–3984 (In Chinese).

Zheng, B., Huo, H., Zhang, Q., Yao, Z.L., Wang, X.T., Yang, X.F., Liu, H., He, K.B., 2014. High-resolution mapping of vehicle emissions in China in 2008. Atmos. Chem. Phys. 14 (18), 9787–9805. https://doi.org/10.5194/acp-14-9787-2014.

Zheng, B., Zhang, Q., Geng, G., Chen, C., Shi, Q., Cui, M., Lei, Y., He, K., 2021. Changes in China's anthropogenic emissions and air quality during the covid-19 pandemic in 2020. Earth Syst. Sci. Data 13 (6), 2895–2907.

Zhou, Y., Cheng, S., Lang, J., Chen, D., Zhao, B., Liu, C., Xu, R., Li, T., 2015. A comprehensive ammonia emission inventory with high-resolution and its evaluation in the Beijing–Tianjin–Hebei (bth) region, China. Atmos. Environ. 106, 305–317. https://doi.org/10.1016/j.atmosenv.2015.01.069.

Zhou, M., Jiang, W., Gao, W., Gao, X., Ma, M., Ma, X., 2021. Anthropogenic emission inventory of multiple air pollutants and their spatiotemporal variations in 2017 for the Shandong province, China. Environ. Pollut. 288, 117666 https://doi.org/10.1016/j.envpol.2021.117666.